ISSN 0001-4370, Oceanology, 2018, Vol. 58, No. 3, pp. 340–349. © Pleiades Publishing, Inc., 2018.
Original Russian Text © N.F. Dimitrieva, Yu.D. Chashechkin, 2018, published in Okeanologiya, 2018, Vol. 58, No. 3, pp. 358–368.

MARINE PHYSICS

Fine Structure of a Stratified Flow around a Fixed and Slow-Moving Wedge

N. F. Dimitrieva[a], * and Yu. D. Chashechkin[b], **

[a] *Institute of Hydromechanics, National Academy of Sciences of Ukraine, Kiev, 03057 Ukraine*
[b] *Ishlinsky Institute for Problems in Mechanics, Russian Academy of Sciences, Moscow, 119526 Russia*
**e-mail: dimitrieva@list.ru*
***e-mail: chakin@ipmnet.ru*

Received April 26, 2016

Abstract—The dynamics of the establishment and spatial structure of flows of a continuously stratified fluid around a fixed and slow-moving horizontal wedge are studied using direct numerical simulation based on the fundamental system of inhomogeneous fluid mechanics equations. Large-scale components (eddies, internal waves, and the wake) and fine-structure components are isolated in the flow patterns in near and away from the obstacle. The mechanism of formation of the propulsive force generating the self-motion of a free body at a neutral-buoyancy horizon is determined. The dependence of the flow parameters on the shape of the obstacle is shown. The transformation of the medium perturbation field at the beginning of the induced slow movement of the wedge at the neutral-buoyancy horizon is traced. The complex structures of fields of different physical quantities and their gradients are visualized. The intrinsic temporal and spatial scales of the flow components are identified.

DOI: 10.1134/S0001437018030050

INTRODUCTION

In the Earth's hydrosphere and atmosphere, stably stratified layers are often observed, which occur under the action of directed heat and salinity fluxes (heating from above and flowing of denser layers from below) and gravitational stratification of media with different densities. In the hydrosphere, the stratification parameters $\rho(z)$ are determined by the corresponding distributions of temperature $T(z)$ and salinity $S(z)$, since the effect of pressure can be ignored when studying small-scale flows due to the low compressibility of water.

Since a nonequilibrium medium can be at rest only when the density gradient is parallel to the line of gravity [6], any perturbing factors—both dynamic factors due to external forces and geometric factors related to the effect of the boundary conditions on the value and direction of flows—violate the conditions of hydrostatic equilibrium and result in the formation of flows. In particular, the no-flow condition for matter on an inclined solid wall results in horizontal inhomogeneity of the background molecular flow of the stratifying component. Deviations of isopycnals from the equilibrium level in the near-boundary regions form horizontal pressure gradients, which accelerate the fluid.

The first model of diffusion-induced steady flows on an infinite inclined plane was proposed by L. Prandtl to explain the formation mechanisms for mountain (valley) breezes, i.e., thin near-boundary jets in a stably stratified atmosphere [8]. As applied to the hydrosphere, the idea was later developed by O. Phillips, who showed the possibility of observing near-boundary flows in a resting stratified fluid in the laboratory [21], and by a number of other scientists, who studied the properties of flows of this type in both stratified and rotating fluids [15]. The influence of boundary effects on the general ocean dynamics is discussed in [14].

The first models of diffusion-induced flows on a topography were developed in a simplified statement: the flow was assumed to be steady, and the bounding surface was assumed to be planar and infinite [8, 21]. In this case, the profiles of velocity and salinity perturbations proved similar and of the same scale. The applicability conditions for the asymptotic method used do not allow flows to be calculated for small boundary inclinations.

Taking into account the variable nature of stratification in real conditions, scientists began to study establishment problems in addition to stationary problems. First, asymptotic solutions to the problem of flow formation on an inclined infinite plane and in a wedge-shaped depression were constructed [17]; then, exact solutions were obtained [4, 5]. In nonstationary flows, the scales of variability of the velocity and salinity pro-

files, which are determined by the kinematic viscosity and diffusion coefficients, considerably differ.

Interest in studying diffusion effects is due to the prevalence of stratified boundary flows that form in lakes, reservoirs, seas, and oceans even in the absence of external force factors [3]. Particular attention is paid to studying slope flows in the atmosphere, where the wind velocity can attain large values on glaciers [19] and in deep mountain valleys [16]. Integrated analytical-numerical models were used to evaluate the effect of sites with distinct properties on the general pattern of valley breezes [22].

Advances in computer technology and programming have made it possible to extend this class of problems, which include diffusion-induced flows around finite-size obstacles placed deep in a stratified medium. Calculations of flow patterns around an immersed sphere and horizontal and inclined finite-length plates based on fundamental fluid mechanics equations agree satisfactorily with the shadow visualization data in laboratory units [1, 23]. Flows of this type around symmetric bodies do not form propulsive forces and moments.

Meanwhile, it was established experimentally that inhomogeneous pressure gradients in diffusion flows acting on obstacles asymmetric with respect to the line of gravity are quite large and can generate self-motion of free bodies at neutral-buoyancy horizons. The self-motion of a wedge-shaped body (diffusion fish) was observed in both single-component stratification [9] and a layered medium with temperature gradients under the action of convection [18]. A diffusion-induced stationary flow around a wedge in a homogeneously stratified medium was calculated in [20].

The steadily increasing interest in studying diffusion-induced flows in recent years is due to the expansion of biohydrodynamic research, in particular, searching for the biolocomotion mechanisms of minute organisms that ensure the collective behavior of large aggregations [13]. In simulating bioprocesses, it is necessary to study the patterns of the fields of physical quantities of objects either at rest with respect to the environment or slowly moving. As experiments show, when an obstacle starts moving, the pattern of the stratified flow changes radically: nonstationary leading and attached internal waves occur, some amount of fluid is blocked ahead of the obstacle, and a trailing wake characterized by a pronounced fine structure forms [11]. The geometry and modes of the flow significantly depend on the properties of the medium and the shape and velocity of the obstacle. It is particularly interesting to study the establishment processes in a unified formulation of the problem with a wide range of parameters without involving additional hypotheses, relationships, and parameters.

The aim of this study is to calculate the dynamics of the establishment of a fine structure of stratified flows around fixed and slow-moving asymmetric obstacles using direct numerical simulation based on the fundamental system of inhomogeneous fluid mechanics equations with allowance for diffusion effects.

1. FORMULATION OF THE PROBLEM AND METHOD OF SOLUTION

We consider the 2D nonstationary problem of establishment of a flow around an immersed obstacle based on the fundamental system of equations including the continuity equation and the momentum and matter transfer equations [6] in the Boussinesq approximation; the effects of compressibility are neglected due to small fluid velocities when compared to the sound velocity. As an equation of state, we take the unperturbed density profile $\rho(S_0(z))$, which is specified by the salinity profile $S_0(z)$ (the z axis is directed upward):

$$\rho = \rho_{00}\left(\exp\left(-z/\Lambda\right) + s\right), \quad \operatorname{div}\mathbf{v} = 0,$$
$$\frac{\partial \mathbf{v}}{\partial t} + (\mathbf{v}\nabla)\mathbf{v} = -\frac{1}{\rho_0}\nabla P + \nu\Delta\mathbf{v} - s\mathbf{g}, \qquad (1)$$
$$\frac{\partial s}{\partial t} + \mathbf{v}\cdot\nabla s = \kappa_s\Delta s + \frac{V_z}{\Lambda},$$

where $S = S_0(z) + s$ is the total salinity including the salt compression coefficient and $s(x,z,t)$ is its perturbed component; ρ_0 is the density at the zero level (at the neutral-buoyancy horizon); $\mathbf{v}$ is the fluid velocity vector; P is pressure minus hydrostatic pressure; ν and κ_s are the kinematic viscosity and salt diffusion coefficients, respectively, which are assumed to be constant; t is time; g is gravitational acceleration; ∇ and Δ are the Hamilton and Laplace operators, respectively; and $\Lambda = \left|d\ln\rho/dz\right|^{-1}$ is the scale, $N = \sqrt{g/\Lambda}$ is the frequency, and $T_b = 2\pi/N$ is the period of buoyancy.

At the initial time moment $t = 0$, an impermeable obstacle is placed in a continuously stratified fluid at rest. On the surface of the obstacle, we have the no-slip condition for velocity and the no-flow condition for matter:

$$\mathbf{v}, s\big|_{t\le 0} = 0, \quad \mathbf{v}\big|_\Sigma = 0, \quad \mathbf{v}, s\big|_{x,z\to\infty} = 0,$$
$$\left.\frac{\partial S}{\partial \mathbf{n}}\right|_\Sigma = -\frac{1}{\Lambda}\frac{\partial z}{\partial \mathbf{n}} + \left.\frac{\partial s}{\partial \mathbf{n}}\right|_\Sigma = 0, \qquad (2)$$

where $\mathbf{n}$ is the external normal to the body surface Σ. At a long distance from the obstacle, we prescribe the attenuation conditions for all perturbations [10].

The solution to problem (1) with boundary conditions (2) describes diffusion-induced flows around a fixed obstacle [23]. The calculated fields of physical quantities are taken as the initial data in the problem of

Table 1. Values of input parameters

Notation	Description	Value
ρ_{00}	Density at zero level, kg/m^3	1020
ν	Kinematic viscosity coefficient, m^2/s	10^{-6}
κ_s	Salt diffusion coefficient, m^2/s	1.41×10^{-9}
N	Buoyancy frequency, s^{-1}	1
g	Acceleration of gravity, m/s^2	9.8
U	Incoming flow velocity, m/s	10^{-5}
L	Wedge length, m	0.1
h	Height of the wedge base, m	0.02

a homogeneous flow of a continuously stratified fluid around an obstacle with velocity U:

$$v_x\big|_{x,z\to\infty} = U, \quad v_z\big|_{x,z\to\infty} = 0. \tag{3}$$

Along with the fundamental equations, the theories of turbulence, boundary-layer approximation, and stationarity are widely used in practice [6, 14, 20]. Group-theoretical analysis has shown that system of equations (1) is consistent with the basic physical principles from which the governing equations are derived, unlike many common constitutive or reduced systems [2]. The introduction of semiempirical hypotheses and relationships restricts the possibility of using models whose continuous symmetries differ from the symmetries of the fundamental equations [2]. Using Reynolds averaging for physical variables results in smoothing of the fine structure of flows. The patterns of steady [8, 14, 21] and nonstationary [4, 17] diffusion-induced flows on an inclined plane distinctly differ even for large times.

System (1), the dimensional parameters of which are given in Table 1, is characterized by a set of time scales including the buoyancy period T_b and the intrinsic time determined by the length and velocity of the body: $t_p = L/U$. The linear scales characterize the unperturbed stratification $\Lambda = \left|d\ln\rho/dz\right|^{-1}$ ($\Lambda = 9.8$ m in a laboratory experiment) according to the size of the obstacle ($L = 0.1$ m) and the length of the attached internal wave $\lambda_i = UT_b$ [11].

Microscales with a dissipative nature (the viscous scale $\delta_N^\nu = \sqrt{\nu/N} = 10^{-3}$ m and the diffusion scale $\delta_N^{\kappa_S} = \sqrt{\kappa_S/N} = 3.8\times10^{-5}$ m) characterize the transverse sizes of the fine-structure components. With a source velocity of $U = 0.001$ cm/s, the length of the attached internal wave $\lambda_i = UT_b = 6.3\times10^{-5}$ m is within the range of microscales. The components of structures with the Prandtl scale $\delta_U^\nu = \nu/U = 10$ m are outside the range of scales under consideration. The Peclet scale $\delta_U^{\kappa_s} = \kappa_s/U = 1.3\times10^{-2}$ cm can be expressed in terms of dimensions of the elements of wake structures.

The wide range of values of the linear scales of the problem (six orders of magnitude) indicates the complexity of the internal structure of a stratified flow, which should be taken into account when developing programs. Analysis of solutions to the linearized fundamental equations and the results of laboratory simulation have shown that large-scale elements of flows (waves and eddies) are characterized by uniformly perturbed components of the complete solution with scales L and λ_i [11]. The geometry of the fine-structure elements of flows, which occur in the entire range of the parameters of the processes under consideration, is described by the elements of a wide family of singularly perturbed components with scales $\delta_N^\nu, \delta_N^{\kappa_S}, \delta_U^\nu, \delta_U^{\kappa_S}$. The fine-structure components affect matter transfer, the processes of separation of matter, and even the increase in the local concentrations in certain regions of the flow [12]. Due to the nonlinearity, individual components actively interact with each other. Interactions of different-scale components for high velocities of the obstacle transform the flow into a nonstationary one [7].

In the nonlinear formulation, system (1)–(3) makes it possible to simultaneously study all elements of flows within a unified description using natural physical variables without additional constants and relationships. Due to the existence of many scales, numerical simulation is one of the main tools to analyze evolving processes.

In the complete nonlinear formulation, a solution to system (1) was constructed numerically by the finite volume method using the freeware OpenFOAM (Open Field Operation and Manipulation). At the heart of its source code is a collection of libraries offering tools to solve a number of applied problems, as well as to perform parallel calculations in supercomputer systems. Numerical simulation of stratified flows around fixed and uniformly moving bodies using the OpenFOAM package showed good performance [23].

However, the standard toolkit of the package includes no program for constructing solutions to system of fundamental inhomogeneous fluid equations (1), which made it necessary to develop an extended numerical model. To take the effects of stratification and diffusion into account, the standard icoFoam solver, which simulates nonstationary flows of a homogeneous fluid, was supplemented with new variables (ρ and s) and the corresponding equations, as well as new auxiliary parameters (N, Λ, κ_s, and g).

The calculation domain is a rectangle in which a symmetric wedge of length $L = 10$ cm and base height $h = 2$ cm is placed horizontally. The lateral sides of the body are arcs of circles; Table 2 gives their radii and positions of centers in the Cartesian coordinate system

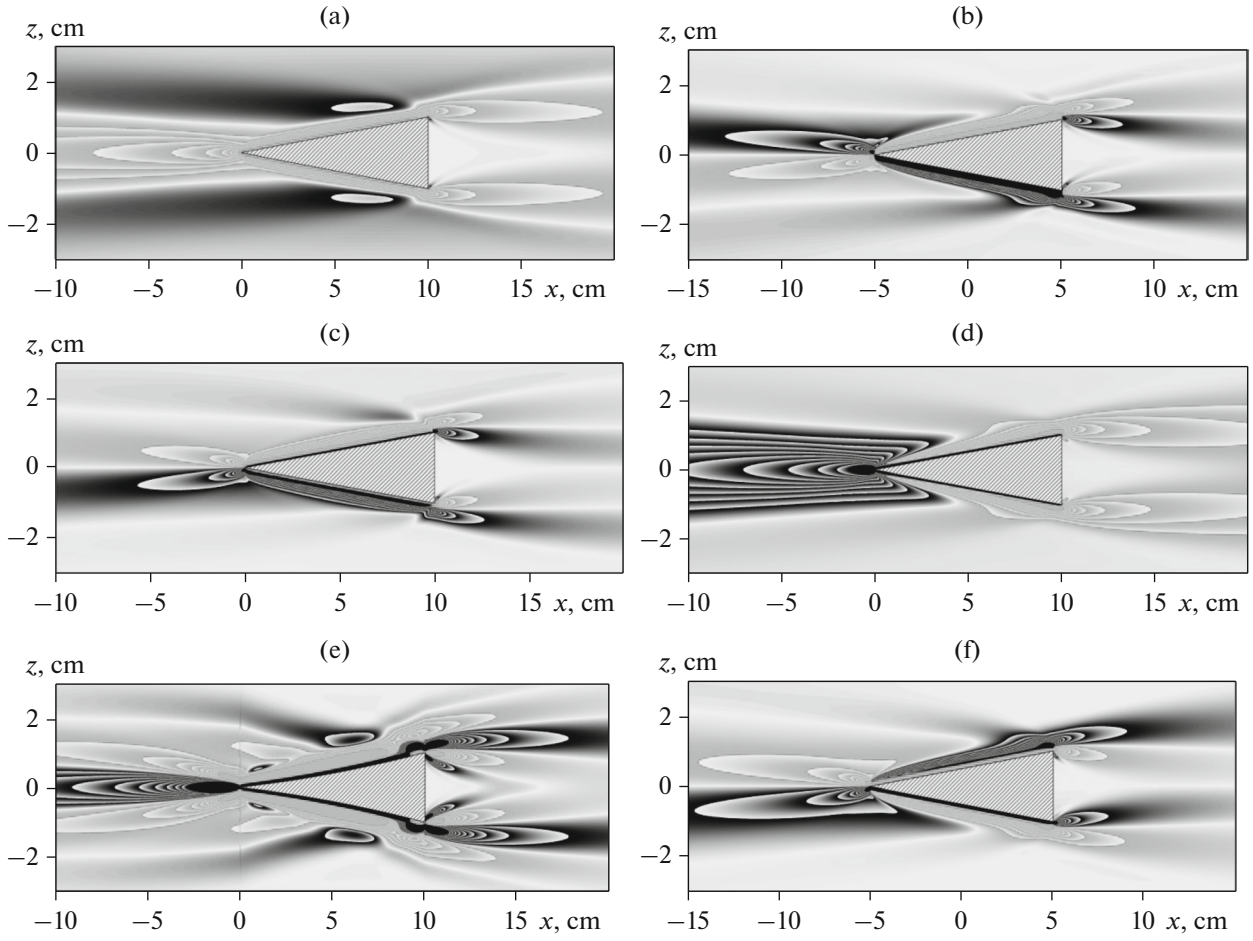

Fig. 1. Perturbation fields in diffusion-induced flow around fixed wedge with right faces (L = 10 cm, h = 2 cm, T_b = 6.28 s, $\tau = t/T_b = 16$) of (a) the longitudinal v_x and (b) vertical v_z velocity components, (c) vorticity, (d) pressure P, and (e) the horizontal $\partial P/\partial x$ and (f) vertical $\partial P/\partial z$ gradient components.

with the origin at the tip of the wedge. With allowance for the shape of the body, a block-structured hexahedral grid is constructed with lines superposed at the boundaries of the blocks. The algorithm for partitioning the calculation domain involves clustering of cells toward the obstacle to resolve thin flow components in regions with large gradient values.

The problems were calculated in parallel using the resources of the UniHUB virtual computing laboratory (www.unihub.ru) and the Lomonosov supercomputer of the Scientific Research Computing Center, Moscow State University (www.parallel.ru).

Table 2. Geometry of wedge

	Coordinates of center, cm	Radius of curvature, cm	Deviation of chord from face Δ_R, cm
1	(−7.6; 126.7)	126.9	−0.1
2	(17.6; 125.7)	125.7	0.1
3	(9.2; 41.4)	43.2	0.3
4	(5.8; 126.7)	10.0	1.4

2. RESULTS OF CALCULATIONS

The calculated patterns of the fields of physical variables illustrate the complex spatial structure of even slow diffusion-induced flows around a wedge, including the thin main jets along the inclined sides, adjacent compensation counterflows, and small-scale perturbations near the sharp edges. The field of the horizontal velocity component is symmetric with respect to the central horizontal plane; see Fig. 1a, where positive and negative values of the visualized quantity are marked, respectively, by light and dark gray. The difference of the values between the isolines is the same.

A more complex flow structure occurs in the field of the vertical velocity component, which illustrates ascending and descending flows (Fig. 1b). The main

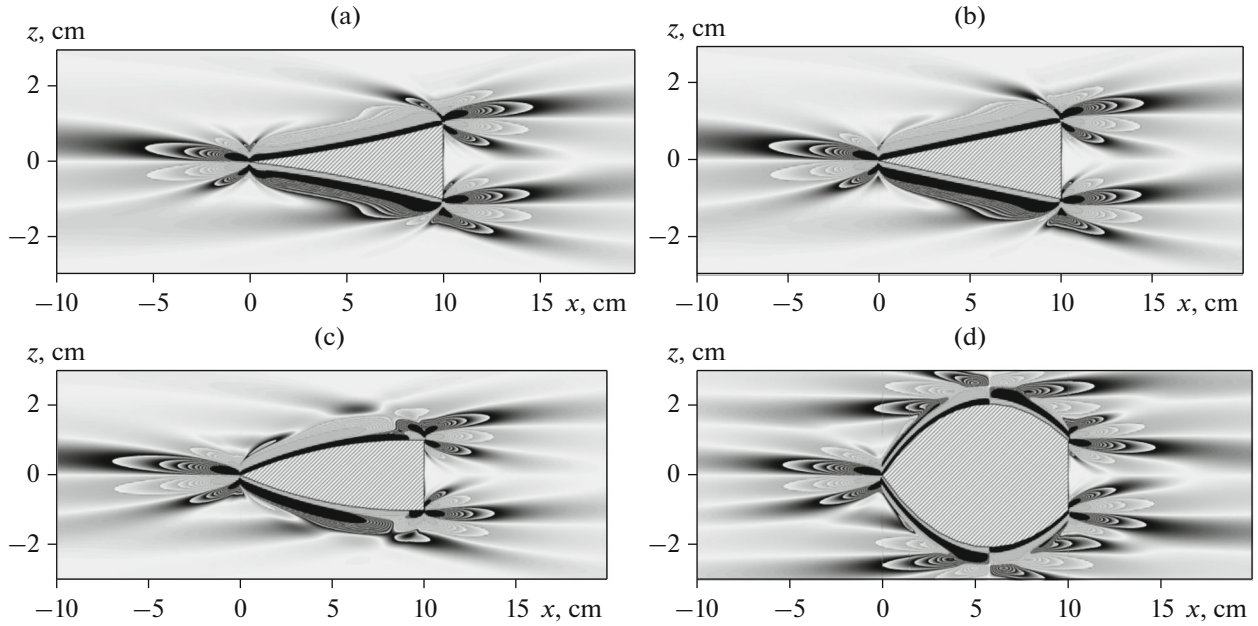

Fig. 2. Effect of body shape on pattern of field of horizontal component of salinity gradient perturbation $\partial s/\partial x$ around fixed wedge ($L = 10$ cm, $h = 2$ cm, $T_b = 6.28$ s, $\tau = t/T_b = 16$) with (a) concave sides, $D_R = -0.1$ cm; (b) right sides, $D_R = 0$ $\Delta_R = 0$; and convex sides for (c) $D_R = 0.3$ cm and (d) $D_R = 1.4$ cm.

jets are detached from the surface at the corner points of the base of the wedge and form a system of dissipative gravity waves. A lengthy unperturbed region adjoins the middle part of the base of the wedge, since the vertical surface does not disturb the homogeneity of background diffusion impurity transfer.

The complexity of the multilevel system of circulation cells adjacent to the sharp edges of an impermeable obstacle immersed in a fixed stably stratified fluid is illustrated by the vorticity field (Fig. 1c). A thin fluid layer with cyclonic (counterclockwise) vorticity directly adjoins the lower face of the wedge. It is followed by a set of alternating compensation areas with different directions of fluid rotation. The vorticity value decreases with distance from the obstacle; conversely, the layer thickness increases. The vorticity distribution in the upper and lower half-planes is antisymmetric with respect to the neutral-buoyancy horizon.

In the pressure field, there is a deficit at the sharp tip of the wedge-shaped obstacle, as well as in the thin layer along the lateral sides (Fig. 1d), where its magnitude decreases monotonically from the sharp tip to the base. The fine structure of stratified flows is pronounced; the pressure values change abruptly here. Near the corner points of the wedge, additional fine-structure components form: dissipative gravity waves.

The area of the pressure deficit extends far forward along the neutral-buoyancy horizon. The difference in pressures acting on the lateral surfaces and base of the body forms an integral force pushing the horizontal wedge toward the tip, which is consistent with observations [17, 19]. The pressure deficit is due to the fact that the fluid is drawn into the ascending structured compensation flow on the upper side and the analogous descending flow on the lower side with stagnation at the bottom of the wake.

The areas with relatively slow parameter changes are separated by thin boundaries with high gradients of the governing physical quantities, in particular, pressure (Figs. 1e and 1f). The maxima of the longitudinal and vertical components of the pressure perturbation gradient near the wedge were about 0.2 Pa/m; the pressure perturbation values were on the order of 10^{-4} Pa. With distance from the obstacle, the pressure perturbation gradient drops abruptly to values of $|\partial p/\partial x| \sim 10^{-5}$ Pa and $|\partial p/\partial z| \sim 10^{-4}$ Pa at a distance from the vertices of the wedge of 5 cm along the horizontal and 0.25 cm along the vertical.

The complex multiscale structure of diffusion-induced flows is also illustrated by the field of the horizontal component of the salinity perturbation gradient (Fig. 2). Near the vertex points of the wedge, additional fine-structure components, dissipative gravity waves, form; in these, the salinity perturbations s were on the order of 10^{-5} and the maxima of the longitudinal component of the salinity perturbation gradient were $|\partial s/\partial x|_{\max} = 4\times10^{-2}$ 1/m.

The pattern of the field of the horizontal component of the salinity perturbation gradient depends on the sign of the curvature of the lateral surface: the

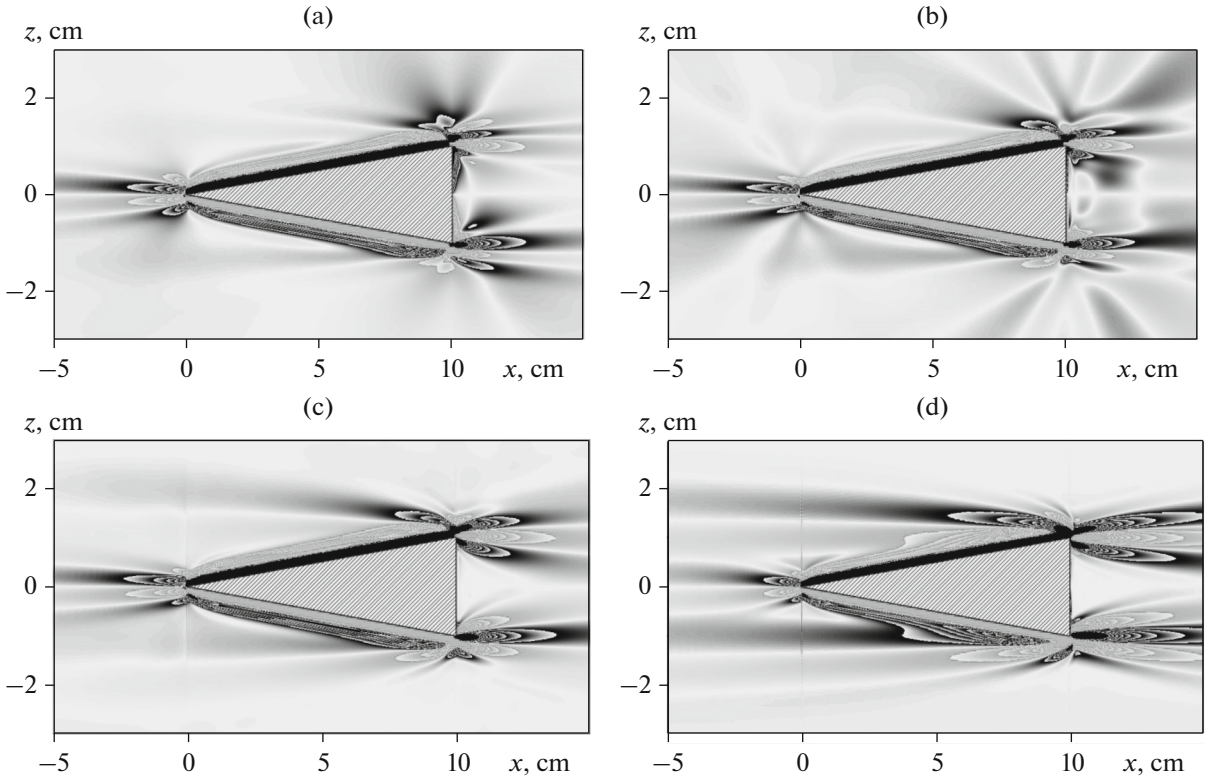

Fig. 3. Evolution of field of horizontal component of salinity perturbation gradient at beginning of movement of right wedge (T_b = 6.28 s, L = 10 cm, h = 2 cm, U = 0.001 cm/s) for (a)–(d) $\tau = t/T_b$ = 0.5; 2; 10; 50.

sharper the vertices of the base the wedge, the more pronounced the alternating strips (Fig. 2a). At the same time, the maximum values $\left|\partial s/\partial x\right|_{\max}$ weakly depend on the curvature of the faces of the wedge. For a convex wedge (Fig. 2c) such that the angle between the base and the lateral face approaches 90°, the beam of fine-structure elements widens. When the vertical of the maximum wedge height does not coincide with the base, the pattern of the flow demonstrates additional fine structures near the poles (Fig. 1d), like those around a sphere [1].

The resulting flow fields around a fixed obstacle were used as an initial condition in the problem of flow establishment when the wedge starts moving at a constant velocity U of 0.001 cm/s, which somewhat exceeds the velocity of wedge self-motion in a stratified medium ($U = 2.83 \times 10^{-4}$ cm/s) [9].

When the wedge starts moving, the flow pattern completely transforms and new structural components occur: leading perturbations, rosettes of nonstationary internal waves, fields of attached internal waves, and a lengthy wake behind the body (Fig. 3). However, at small Reynolds numbers, when the source velocity U is comparable to the typical velocity of diffusion-induced flows $U_N^{\kappa_S}$, specified nonzero initial conditions manifest themselves in a sufficiently long flow structure (about $20T_b$). The main changes occur near the tip and vertex points of the base of the wedge, where nonstationary internal waves begin to form. The phase surfaces (the boundaries of the radial strips in Fig. 3a) are somewhat asymmetric even at the initial stage: the beams directed along the movement of the wedge are brighter than the reversed ones. With time, the minimum slope of the beams of nonstationary waves decreases and the length increases. Extended beams become a dominant element of the flow pattern in Fig. 3b.

Simultaneously with the long waves, a group of shorter high-amplitude waves forms at the trailing edge, including both direct waves facing the movement of the wedge and backward waves oriented to the start point (backward waves are not recorded when the body moves at higher velocities [11]). With increasing amplitude, the wave pattern at the edges of the body becomes more pronounced and the beams become longer (Fig. 3c). The wave component of the flows becomes dominant and perturbs the flow structure at the lateral surfaces of the wedge.

For long times, the almost steady pattern of the flow includes a group of relatively large leading internal waves (the system of sloping strips in Fig. 3d), which are forward-oriented perturbations at the leading edge of the body, and a system of waves near the

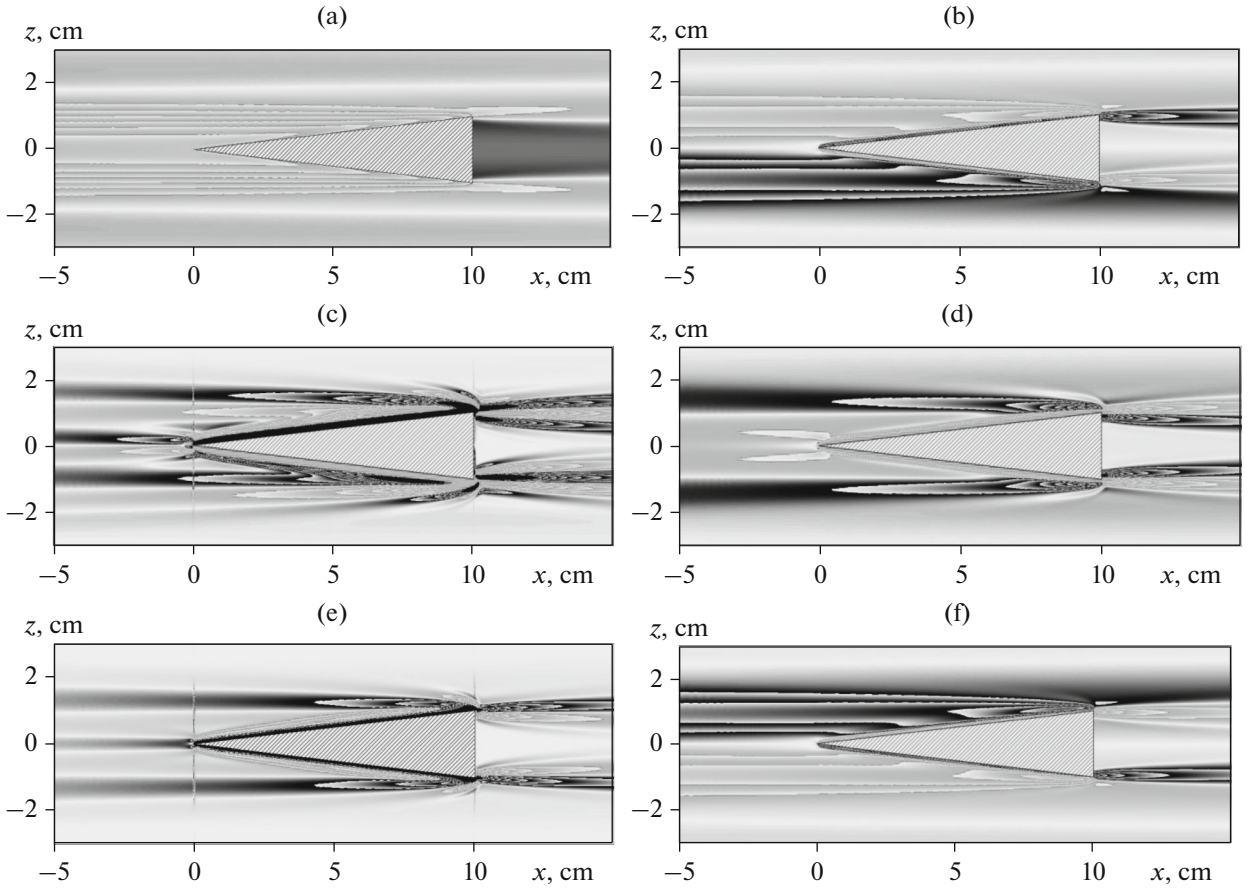

Fig. 4. Perturbation fields around moving wedge ($L = 10$ cm, $h = 2$ cm, $T_b = 6.28$ s, $U = 0.001$ cm/s, $\tau = t/T_b = 100$) of (a) pressure P, (b) salinity s, (c) longitudinal $\partial s/\partial x$ and (d) vertical $\partial s/\partial z$ components of salinity gradient, and (e) longitudinal $\partial P/\partial x$ and (f) vertical $\partial P/\partial z$ components of pressure gradient.

vertices of the base, which are oriented forward and backward along the wedge movement. The density distribution remains unperturbed in the central part of the trailing wake, which the reversed wave beams do not enter. The number of observed waves that do not enter the wake behind the body increases with time.

The waves noticeably deform the layered flow at the lateral sides of the wedge. The flow continues to evolve slowly with time: the perturbation amplitudes increase, and the slopes of the main wave strips decrease. Their extensions intersect the x axis at the starting point of the body.

The flow patterns around the wedge agree with the results of independent calculations [7] and with the visualization patterns of the distribution of the gradient of the refractive index in a laboratory tank for bodies with other geometric shapes [11] (the color-shadow method with a horizontal slit and grating).

The pattern of the perturbation fields for a stratified fluid with a wedge slowly moving at a velocity of $U = 0.001$ cm/s is specific for each physical parameter. The field of pressure perturbations has the simplest geometry: there is an excess in a layer in the entire half-space ahead of the obstacle and outside the wake behind the obstacle, as well as a deficit in the rectangular wake (*underpressure* according to the terminology of P. du Buat). Areas of perturbations with other signs adjoin the main strips in the entire flow from the outside. The height of the wake is slightly less than the size of the base of the wedge. Near the vertices of the base, there are weakly pronounced short internal waves whose phase surfaces are oriented opposite to the direction of movement (Fig. 4a).

The salinity perturbation field also has a global striped structure; its isolines tend to approach the lateral surface of the wedge along the normal (Fig. 4b). However, the smooth nature of the curves is violated in a thin near-surface flow. Small-scale perturbations oriented toward and opposite the flow and are pronounced at the vertices of the base. Behind the body, short waves enter the density wake. In general, the pattern of the salinity field is antisymmetric with respect to the central horizontal plane, in contrast to the pressure field.

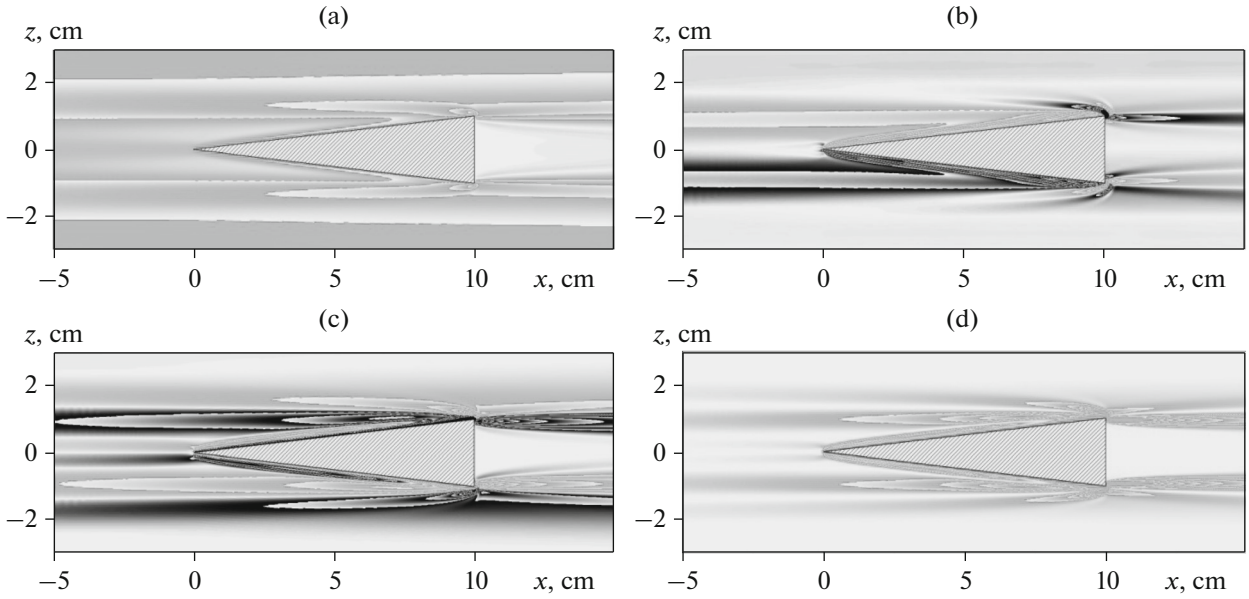

Fig. 5. Perturbation fields around moving wedge ($L = 10$ cm, $h = 2$ cm, $T_b = 6.28$ s, $U = 0.001$ cm/s, $\tau = t/T_b = 100$) of (a) longitudinal v_x and (b) vertical v_z velocity components, (c) vorticity, and (d) dissipation rate of mechanical energy.

The field of the horizontal component of the salinity gradient, which has an inhomogeneous zero value in the unperturbed medium, is characterized by the most complex structure: all components of the complicated field of internal waves are present (Fig. 4c). A relatively long-wave component occurs (straight strips with a wavelength of $\lambda_w = 1.3$ cm and with shorter wavelengths of $\lambda_w = 0.2$ cm near the vertices, and of $\lambda_w = 0.6$ cm near the tip of the wedge). The strips near the lateral sides of the wedge visualize a complex alternating pattern of perturbations, which is typical of nonstationary flows near inclined surfaces [5, 8, 17, 21, 23].

The patterns of the fields of the salinity gradient components show most completely the fine structure of the fields of internal waves that form for a moving a wedge (Figs. 4c and 4d). The field of the gradient horizontal component is antisymmetric with respect to the central plane of the wedge, which is due to the nature of the displacement of fluid layers. The field of the vertical component is symmetric: first, the layers forced away by the wedge forming the equilibrium horizons are constricted and the gradient increases; then, the layers are stretched, and the gradient decreases. The physical quantity of the gradients reflecting the inhomogeneity of molecular and advective flows of a stratifying impurity behave nonmonotonically near a streamlined body and attain large numerical values ($|\partial s/\partial x|_{\max} = 3\times10^{-2}$ 1/m, $|\partial s/\partial y|_{\max} = 9\times10^{-2}$ 1/m).

Up to the type of symmetry, the field of the horizontal component of the pressure gradient (Fig. 4e) is reproduced by the structure of the field of internal waves represented in the salinity field (Fig. 4c); however, the perturbations near the tip of the wedge are less pronounced here.

Up to symmetry, the pattern of the field of the vertical component of the pressure gradient (Fig. 4f) is similar to the field of salinity perturbations (Fig. 4b) with a clear deviation of the isopleths in the direction of the normal to the impermeable surface of the body.

In the pattern of the horizontal component of the velocity field, there is a unidirectional flow toward the base (Fig. 5a), whose striped structure is determined by the internal waves, which are more pronounced in Fig. 5b in the field of the velocity vertical component. However, thin perturbations near the tip of the wedge are not visualized here as well.

An even more complex structure is observed in the vorticity field in which there are leading perturbations, jet flows at the lateral faces, and rosettes of internal waves in the neighborhood of the corner points of the body (Fig. 5c). The dynamic components of the flow are most contrasting in the field of the dissipation rate of mechanical energy, the quadratic nature of which relieves the image of excessive detail due to the alternating sign of the other physical quantities (Fig. 5e).

On the whole, examination of the images shows that the inhomogeneity of a flow of a stratifying component near an obstacle forms perturbations in a large region, whose sizes are determined by the efficiency of generation of the entire family of internal waves, both long leading waves and short waves near the wedge vertices. The self-propulsion observed in [9] induces a field of the pressure gradient whose perturbing action

exceeds the friction against the faces of the upward flow from above and of the downward flow from below. The principal difference between the flow patterns around a wedge in homogeneous and stratified fluids manifests itself near the extreme points of the streamlined body. Near acute angles, systems of periodic structures occur, which visualize the field of internal waves.

The source of internal waves is the edge singularities, which generate intense vertical fluid displacement, which leads to displacement of the fluid layers from the initial neutral-buoyancy position and, as a result, to the formation of periodic damped oscillations.

CONCLUSIONS

For the first time, a complete numerical solution to the problem of formation of a diffusion-induced flow around a fixed wedge in a continuously stratified fluid and to the problem of establishment of field patterns when the body starts moving at a small velocity (in the velocity range for the self-motion of a free body at the neutral-buoyancy horizon) is constructed. The fields of the basic physical quantities (velocity, density, vorticity, energy dissipation rate, and the components of the salinity and pressure gradients) are calculated.

The physical mechanism for the self-propulsion of bodies in a stably stratified fluid at rest is the pressure deficit near acute parts of the bodies, because the fluid is drawn into the ascending structured compensation flow on the upper side and the analogous descending flow on the lower side.

In all cases, the patterns of the fields of the physical quantities are characterized by a complex spatial structure reflecting the effect of structural flow components: jets at the boundary of the body, short internal waves near the vertices, and longer internal waves. The finest structures of flows occur near the vertices of the base of the wedge; here, the turning regions for the main jets are sources of dissipative gravity waves, which are visualized in laboratory experiments at extended horizontal striped structures.

The dimensions of the perturbation field are determined by the efficiency of wave generation, which in turn depends on the value of stratification, the dimensions of the body, and its velocity. Large (when compared to the body) sizes of the region of dynamic perturbations ensure the long-range interaction of slow-moving bodies in a stratified fluid, which is likely one of the mechanisms of clustering of small biological objects without special locomotory organs. Natural metabolism that ensures the consumption of certain substances from the environment and the excretion of others can also affect the self-propulsion of the smallest organisms.

A unified approach to calculations makes it possible to use the results from calculating two-dimensional diffusion-induced flows around a fixed obstacle as the initial conditions for the problem of establishment of the flow pattern when a body begins, and then continues, moving at a constant velocity. The resulting flow pattern with a small Reynolds number includes leading perturbations, the wake, and a family of internal waves observed in experiments using high-sensitive shadow apparatus.

ACKNOWLEDGMENTS

This study was supported by the Russian Academy of Sciences (basic research program of the RAS Presidium "World Ocean: Multiscale, Multiphase, Multiparameter") and the Russian Foundation for Basic Research (project no. 15-01-09235).

REFERENCES

1. V. G. Baidulov, P. V. Matyushin, and Yu. D. Chashechkin, "Evolution of the diffusion-induced flow over a sphere submerged in a continuously stratified fluid," Fluid Dyn. **42**, 255–267 (2007).
2. V. G. Baidulov and Yu. D. Chashechkin, "Comparative analysis of symmetries for the models of mechanics of nonuniform fluids," Dokl. Phys. **57**, 192–196 (2012).
3. V. N. Zyryanov and L. E. Lapina, "Slope flows governed by diffusion effects in seas, lakes, and reservoirs," Water Resour. **39**, 294–304 (2012).
4. A. V. Kistovich and Yu. D. Chashechkin, "The structure of the nonstationary boundary flow on an inclined plane in a continuously stratified medium," Dokl. Akad. Nauk **325**, 833–837 (1992).
5. A. V. Kistovich and Yu. D. Chashechkin, "Diffusion induced unsteady boundary flows in a wedge-shaped trough," J. Appl. Math. Mech. **62** (5), 743–748 (1998).
6. L. D. Landau and E. M. Lifshitz, *Course of Theoretical Physics*, Vol. 6: *Fluid Mechanics* (Pergamon, New York, 1987; Nauka, Moscow, 1986).
7. Yu. D. Chashechkin and Ya. V. Zagumennyi, "Structure of the pressure field on a plate in the transient flow regime," Dokl. Phys. **60**, 299–304 (2015).
8. *Prandtl-Führer durch die Strömungslehre: Grundlagen und Phänomene*, Ed. by H. Oertel, Jr. (Vieweg Verlag, Braunschweig, 2001; Regulyarnaya i Khaoticheskaya Dinamika, Moscow, 2007).
9. M. R. Allshouse, M. F. Barad, and T. Peacock, "Propulsion generated by diffusion-driven flow," Nat. Phys. **6**, 516–519 (2010).
10. Yu. D. Chashechkin, "Differential fluid mechanics—harmonization of analytical, numerical and laboratory models of flows," in *Mathematical Modeling and Optimization of Complex Structures*, Computational Methods in Applied Sciences Series **vol. 40** (Springer-Verlag, New York, 2016), pp. 61–91.
11. Yu. D. Chashechkin and V. V. Mitkin, "Vortex arrays past a sloping strip uniformly moving in homogeneous or linearly stratified fluid," J. Visualization **5** (2), 120 (2002).
12. Yu. D. Chashechkin and V. V. Mitkin, "Transportation of a dye in upstream and downstream wakes of the cyl-

inder in continuously stratified liquid," J. Visualization **10** (1), 7 (2007).

13. L. H. Cisneros, R. Cortez, C. Dombrowski, et al., "Fluid dynamics of self-propelled microorganisms, from individuals to concentrated populations," Exp. Fluids **43**, 737–753 (2007).
14. C. Garrett, "Do near-boundary processes control the ocean?" *Proceedings of the 13th Aha Huliko'a Hawaiian Winter Workshop "Near-Boundary Processes and Their Parameterization*" (University of Hawaii, Manoa, 2003), pp. 1–7.
15. C. Garrett, P. MacCready, and P. B. Rhines, "Boundary mixing and arrested Ekman layers: rotating, stratified flow near a sloping boundary," Ann. Rev. Fluid Mech. **25**, 291–323 (1993).
16. C. M. Hocut, D. Liberzon, and H. J. S. Fernando, "Separation of upslope flow over a uniform slope," J. Fluid Mech. **775**, 266–287 (2015).
17. P. F. Linden and J. E. Weber, "The formation of layers in a double-diffusive system with a sloping boundary," J. Fluid Mech. **81**, 757–773 (1977).
18. M. J. Mercier, F. M. Ardekani, M. R. Allshouse, et al., "Self-propulsion of immersed object via natural convection," Phys. Rev. Lett. **112**, 204501(5) (2014).
19. J. Oerlemans and W. J. J. van Pelt, "A model study of Abrahamsenbreen, a surging glacier in northern Spitsbergen," Cryosphere **9** (2), 767–779 (2015).
20. M.A. Page, "Propelled by diffusion," Nat. Phys. **6**, 486–487 (2010).
21. O. M. Phillips, "On flows induced by diffusion in a stably stratified fluid," Deep-Sea Res. **17**, 435–443 (1970).
22. A. Shapiro and E. Fedorovich, "A boundary-layer scaling for turbulent katabatic flow," Boundary-Layer Meteorol. **153** (1), 1–17 (2014).
23. Ia. V. Zagumennyi and Yu. D. Chashechkin, "Diffusion induced flow on a strip: theoretical, numerical and laboratory modeling," Procedia IUTAM **8**, 256–266 (2013).

Translated by N. Berestova